Article

Cancer targeted enzymatic theranostic prodrug: Precise diagnosis and chemotherapy

Weon Sup Shin, Jiyou Han, Peter Verwilst, Rajesh Kumar, Jong-Hoon Kim, and Jong Seung Kim

Bioconjugate Chem., **Just Accepted Manuscript** • DOI: 10.1021/acs.bioconjchem.6b00184 • Publication Date (Web): 02 May 2016

Bioconjugate Chemistry is published by the American Chemical Society. 1155 Sixteenth Street N.W., Washington, DC 20036

Cancer targeted enzymatic theranostic prodrug: Precise diagnosis and chemotherapy

Weon Sup Shin,[†,§], Jiyou Han,[‡,§] Peter Verwilst,[†,§] Rajesh Kumar,[†] Jong-Hoon Kim,[‡,*] Jong Seung Kim[†,*]

[†]Department of Chemistry, Korea University, Seoul 136-701, Korea.

[‡]Department of Biotechnology, Laboratory of Stem Cells and Tissue Regeneration, College of Life Sciences & Biotechnology, Korea University, Seoul 136-713, Republic of Korea.

§ The authors contributed equally.

E-mail: jhkim@korea.ac.kr (J. - H. Kim); jongskim@korea.ac.kr (J.S. Kim)

Abstract

The development of targeted and effective theranostic (therapeutic and diagnostic) chemotherapeutic agents is highly desirable for precise diagnosis and treatment of cancer. To realize this goal, we developed a cancer-targeting and enzyme-triggered theranostic prodrug **1**, containing 7-ethyl-10-hydroxycamptothecin (SN-38), a well-known anticancer drug, which inhibits topoisomerase I in the cell nucleus; hydroquinone as an enzyme-triggered moiety; and biotin as a cancer targeting unit. Enzyme-triggered theranostic prodrug **1** selectively targets cancer cells and is subsequently activated in the presence of NAD(P)H: quinone oxidoreductase-1 (NQO1), a cytosolic flavoprotein that catalyzes the two-electron reduction of quinone moieties with the concomitant consumption of NADH or NADPH as electron donors. High levels of NQO1 were found in a variety of cancer cell lines compared to healthy cells, and therefore, it is an excellent target for the development of cancer targeted drug delivery systems. Upon preferential cancer cell delivery and uptake, aided by biotin, the enzyme-triggered theranostic prodrug **1** is cleaved by NQO1, with the subsequent release of SN-38, inhibiting topoisomerase I, leading to apoptosis. The drug release and induced apoptosis of cancer cells expressing both biotin receptors and

high levels of NQO1 was simultaneously monitored *via* the innate fluorescence of the released SN-38 by confocal microscopy. *In vitro* and *in vivo* studies showed an effective inhibition of cancer growth by the enzyme-triggered theranostic prodrug **1**. Thus, this type of enzyme-triggered targeted prodrug therapy is an interesting and promising approach for future cancer treatment.

Introduction

A lack of specificity of the inherently highly toxic anticancer agents is one of the main obstacles limiting the currently available chemotherapeutic treatment effectivity.[1] Over the course of the last decades, a large variety of prodrugs exploiting the unique cancer microenvironment with increased levels of intracellular thiols,[2-7] significantly lower extracellular pH levels[8] and elevated concentrations of extra- and intracellular reactive oxygen species (ROS)[9] have been developed. However, many of these prodrugs suffer from a vital drawback in that the real-time monitoring of drug activation upon internalization and subsequent localization is not straightforward, even though the detailed understanding of these events is of crucial importance in the development of novel treatments.[10]

The tumor microenvironment not only differs in pH and reductive and oxidative potentials, but as a result of the malignant transformation of healthy tissues to tumors, a whole array of enzymes exhibit differential expression. NAD(P)H:quinone oxidoreductase-1 (NQO1)[11] has recently emerged as a prime candidate for the in situ activation of prodrugs,[12-18] as a number of cancer cells, of widely varying origins, have been found to exhibit strongly elevated NQO1 concentrations (up to ~12 to 50 fold).[19-24]

While the activation of drugs under the particular physiological microenvironment in tumors is a major step towards widening the therapeutic window of anticancer drugs, the targeted delivery of drugs to these tissues has an equally important role to play in reaching that goal. Many membrane bound receptors are overexpressed in cancer cells, and thus have the potential to increase the amount of drugs delivered to these cells. A large variety of small molecules, peptides and proteins and polymers have been studied in recent years.[25,26-27] Amongst these tumor-targeting molecules, vitamins are some of the most effective and practically applicable targeting agents,[26-27] as they generally do not suffer from drawbacks associated with other targeting agents, including poor scalability, production and purification cost, difficulty modifying or substituting, a lack of stability towards metabolic processes and the potential of mounting an (auto)immune response. As rapidly proliferating cells such as cancer cells have an increased requirement for these molecules, receptors mediating vitamin uptake are overexpressed on the cell surface of many cancer cells.[30] Amongst the vitamins, especially the B-vitamins are interesting candidates for drug delivery purposes. The most widely studied are folic acid (vitamin B9), cobalamine (vitamine B12) and biotin (vitamin B7) and recent evidence points towards biotin receptors as the most universally overexpressed in malignant tissues rather than the folate receptor or receptors for cobalamines,[30,31] hence biotin emerged as the logical choice and was thus adopted as a targeting agent in the current project.

Camptothecin, a pentacyclic-quinolone-based natural product, has been shown to exhibit a remarkably potent antiproliferative action in cancer cells due to the inhibition of topoisomerase I. Two (semi)synthetic analogues, exhibiting better solubility and pharmacokinetic profiles, topotecan and irinotecan, have been approved by the US Food and Drug Administration and are currently used in clinical practice.[32] The active metabolite (SN-38) of camptothecin, exhibiting a significantly higher cytotoxicity than the parent compound,[33] is an ideal drug to study the real-time monitoring of drug delivery and in situ activation, as the compound has an intrinsic fluorescence in the free, but not the conjugated form, thus representing a definite advantage over non-fluorescent prodrugs. As a recent paper by Liu et al. shows, the combination of an NQO1 activatable trigger and pentacyclic-quinolone-based drugs represents a particularly powerful prodrug combination in vitro,[34] but is likely to fail to show the same remarkable effect in vivo for the lack of a targeting group.

For the reasons outlined above, we designed a novel tumor-targeting masked enzyme-triggered theranostic prodrug 1 consisting of three parts (Scheme 1). A biotin conjugate acts as a cancer-targeting unit that draws the antitumor agent to cancer cells with high selectivity. The second part is an enzyme-activatable unit,[12-17] a quinone propionic acid which also acts as a strong quencher of fluorescence. The crucial third component of this molecular triad is the cytotoxic anticancer drug, SN-38, which allows for a strong anticancer effect as well as doubling as a fluorescent group for imaging and monitoring.

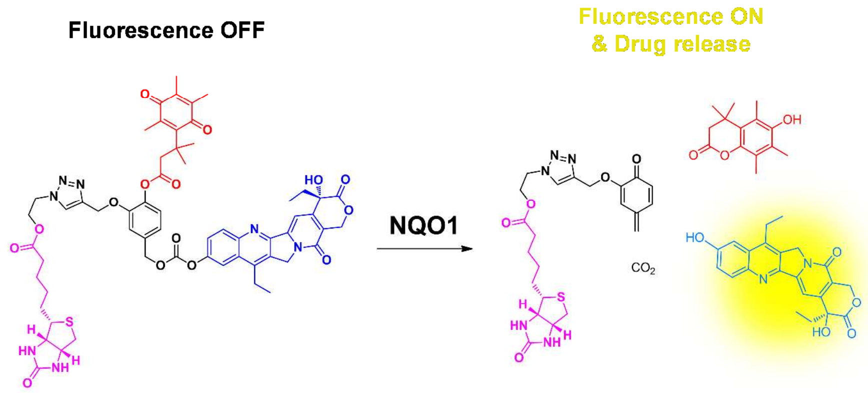

Scheme 1. Proposed drug release mechanism.

Results and discussion

The synthesis of **1** is described in Scheme 2. Compounds **7**, **8** and **9** were synthesized by previously reported methods.[8,35,36] Compound **6** was obtained after a simple reduction using sodium borohydride. After this reduction, compound **6** was reacted with tert-butyldimethylsilyl chloride to protect the benzylic alcohol, resulting in **5**. Following the subsequent esterification of the phenolic position with the quinone propionic acid (**8**) via an EDCI coupling, the TBDMS group was removed with methanesulfonic acid, allowing for the conjugation of SN-38 via a carbonate bond (**2**). Finally, a click reaction between **2** and **9** yielded the final compound **1**. All new compounds were characterized by ^{1}H and ^{13}C nuclear magnetic resonance (NMR) and electrospray ionization mass spectrometry (ESI-MS; Supplemental Figures S1-16).

To study the behavior of **1** upon exposure to NQO1, the fluorescence of **1** was monitored upon addition of human recombinant NQO1 and NADH, revealing the appearance of a fluorescent band centered at 550 nm, corresponding to free SN-38 (Figure 1a) with the fluorescence at around 450 nm corresponding to NADH fluorescence. Upon the addition of NQO1, the time-course experiment demonstrated full release of SN-38 within 30 minutes with an increase in fluorescence at 550 nm of up to 400% (Figure 1b). As the specificity of the trigger for NQO1 is of primordial importance to the success of the drug delivery system, the fluorescence of **1** was monitored upon the addition of a variety of amino acids and biothiols, showing no or negligible response at 550 nm, in contrast to NQO1 (Figure 1c). Additional evidence to the stability of the probe under physiological conditions was provided by monitoring the fluorescence over a 20 h period in blood serum, demonstrating over 90% unchanged **1** (Figure 1d). The pH dependence on the stability of probe **1** was further demonstrated as depicted in Figures S17-19, showing no or negligible hydrolysis in the absence of NQO1 over the course of two hours, and the clear release of SN-38 as demonstrated from the fluorescence 2h subsequent to the addition of NQO1 and NADPH. The identity of the drug after NQO1 mediated drug release was further confirmed by HPLC analysis (Figure S20).

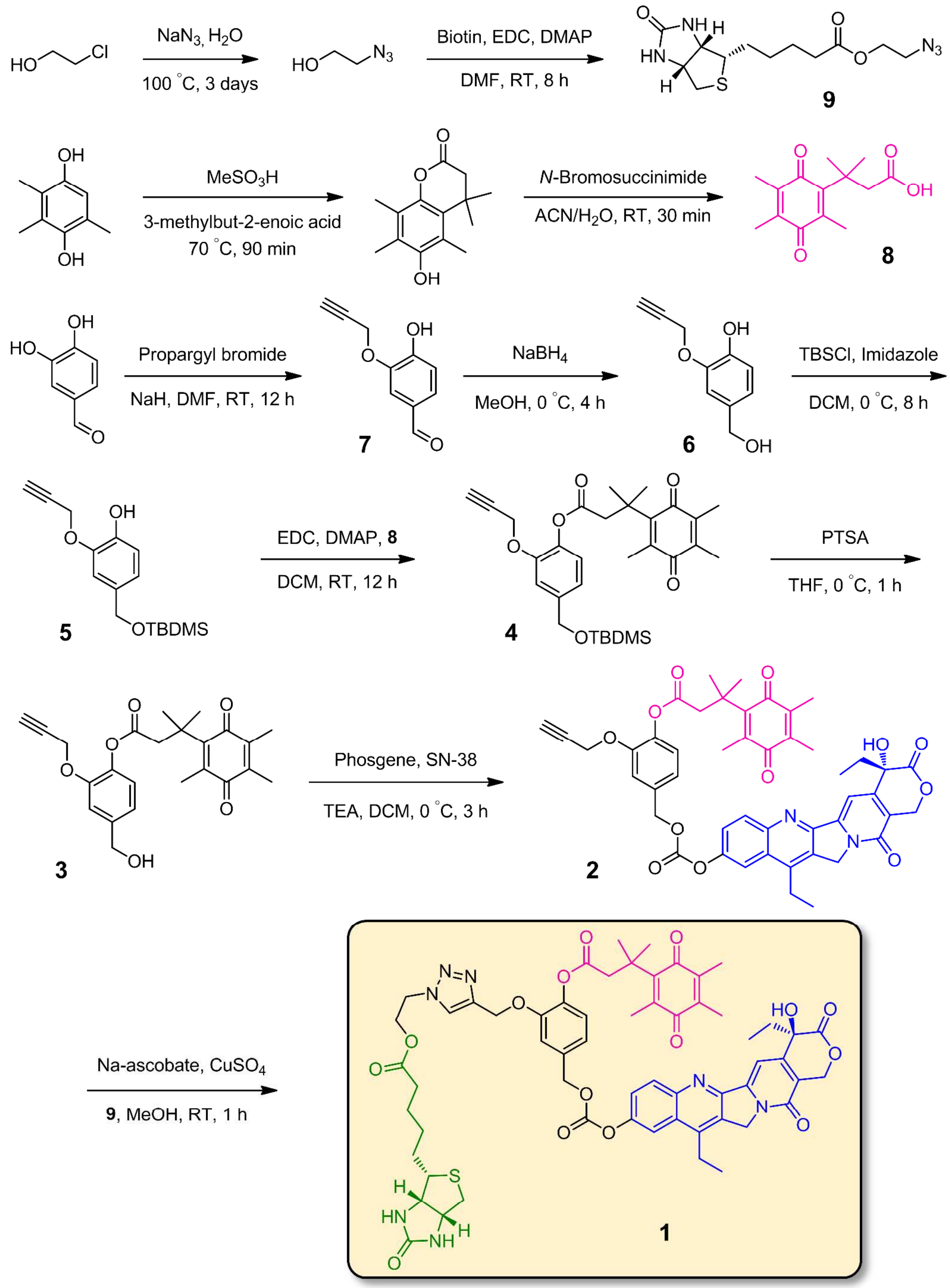

Scheme 2. Synthetic pathway of probe **1**

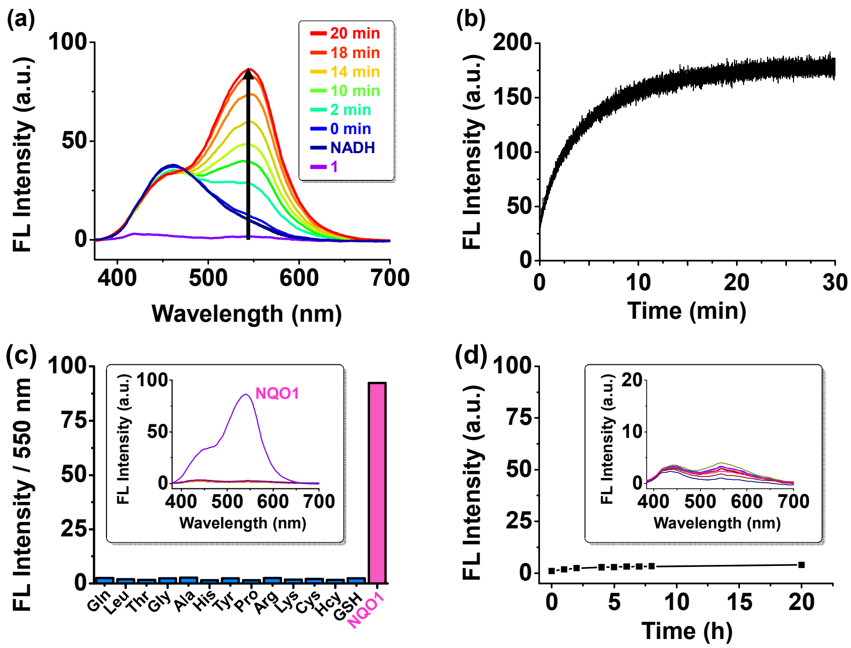

Figure 1. (a) Fluorescence spectra of **1** with NQO1 (40 μg) and NADH (100 μM) in pH 7.4 PBS. (λ_{ex} = 365 nm, Slit = 5/5, sensitivity = low, 25 °C) (b) Changes in fluorescence intensity in pH 7.4 PBS (λ_{ex} = 365 nm, λ_{em} = 550 nm, Slit = 3/3, sensitivity = high, 25 °C) (c) Reactivity of **1** in the presence of other biological amino acids. Fluorescence responses of **1** (20.0 μM) toward 100 μM of amino acids in pH 7.4 PBS (d) stability of **1** (20.0 μM) in serum for 20 h.

Encouraged by these results, the *in vitro* and *in vivo* chemotherapeutic effect of prodrug DDS system **1** was assessed. The cell viability of two cancer cell lines (A549 and HeLa), shown to express the biotin receptor,[31] were significantly decreased, whereas human normal fibroblast cell lines (WI-38 and BJ), lacking significant levels of this receptor,[31] were not affected by prodrug **1** (Figure 2a-b). These results demonstrate the target specificity of prodrug **1** as a result of biotin. Additionally, NQO1 expressed in normal cells is relatively low, and it might be not sufficient to induce apoptosis.[28, 29]

After the *in vitro* cancer specific cytotoxicity was confirmed, we performed *in vivo* experiments to examine the tumor selectivity of prodrug **1**. A549-cell-inoculated xenograft mice were injected with prodrug **1** or SN-38 via tail vein injection. The tumor-specific accumulation and enzymatic release of SN-38 from prodrug **1**, as observed by significant tumor growth retardation, indicates its target specificity (Figure 3a-b). As early as 3 weeks after prodrug **1** injection, significant reductions in tumor volume were observed, compared to the control and SN-38 (Figure 3c). At the end of the experiment, the diagnostic ability of prodrug **1**, evidenced by enhanced fluorescence emission in the solid tumor in comparison to in other organs, was clearly apparent (Figure 3d). These *in vivo* results validate the design strategy for the selective activation of prodrug 1 in tumor tissues, exclusively releasing SN-38 in the presence of biotin and NQO1, and thus achieving tumor growth inhibition. Interestingly, these results furthermore demonstrate the chemotherapeutic effects of prodrug **1** is very effectively maintained over 14 weeks in the *in vivo* system, when repeatedly administered.

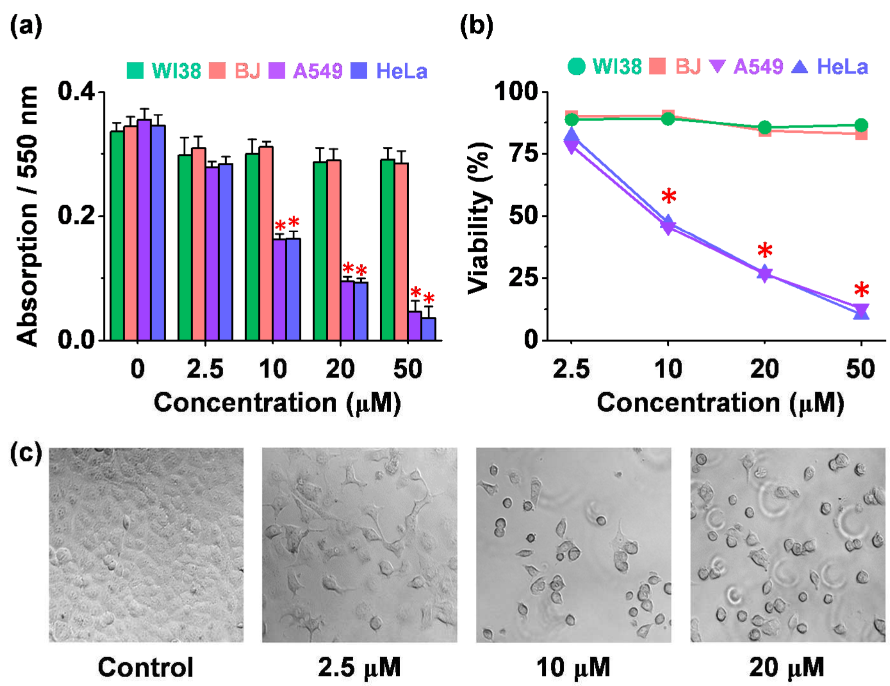

Figure 2. *In vitro* cytotoxicity of prodrug **1**. (a) Cytotoxicity of two cancer cell lines (A549 and HeLa) and two normal cell lines (WI-38 and BJ). (b) Relative percentage of cell viability was presented (*P < 0.05). (c) Phase contrast images of prodrug **1** treated A549 cells at various concentrations. Note that images were taken after 24 h of prodrug **1** treatment. Magnification of (c): 200X.

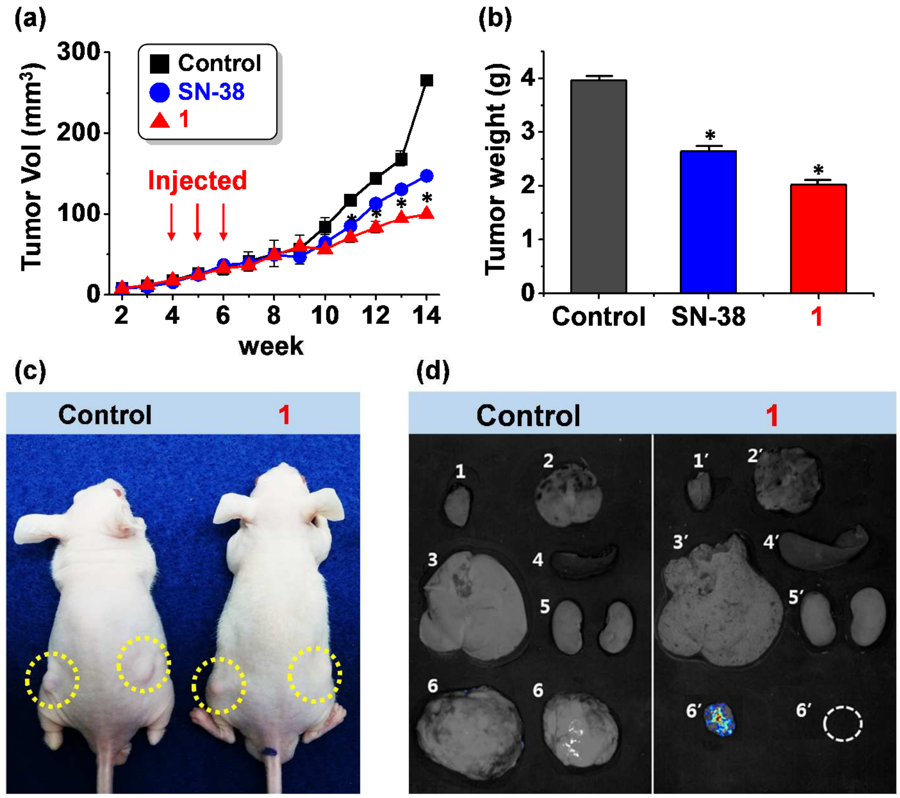

Figure 3. *In vivo* chemotherapeutic effects of prodrug **1** in a xenograft mouse model. (a) Prodrug **1** (3 mg/kg, two times tail-vein injection per week for 3 weeks) affects tumor growth in xenograft mice (n = 4 per treatment). Tumor size gradually decreased upon treatment with **1**. SN-38 (3 mg/kg) treatment was used as a control. (b) The final weight of the tumors at termination (14 weeks) of prodrug-injected xenograft mice was much lower than that of the tumors of control mice (*P < 0.05). (c) *In vivo* visualization of solid tumors in A549-cell-inoculated xenograft mice. (d) Representative *ex vivo* fluorescent image of five major organs; heart (1 and 1′), lung (2 and 2′), liver (3 and 3′), spleen (4 and 4′), kidney (5 and 5′), and tumor (6 and 6’).

NQO1 is expressed mainly in the cytosol, yet recently a few studies have reported that it is also localized in mitochondria, ER, and the nucleus.[37] Accordingly, our fluorescent images obtained from co-localization experiments clearly indicate that a certain amount of NQO1 is expressed in mitochondria, ER and the nucleus (Figure 4a). Based on the merged images (Figure 4a), the fluorescence originating from SN-38 released by prodrug **1** partially overlaps with mitotracker and completely overlaps with ER-tracker. Its expression *in situ* is sufficiently high to trigger prodrug **1** to release the fluorescent SN-38. Furthermore, the gene expression of topoisomerase I was decreased in a dose-dependent manner, as compared to the control as well as SN-38 treated cells (Figure 4b: TPO1). A major obstacle in cancer treatment is multidrug resistance by drug transporters, observed with nearly all commonly used anticancer agents. As one of the major drug transporters, human BCRP (ABCG2) contributes significantly to multidrug resistance in cancer treatment.[38] Interestingly, ABCG2, the major drug transporter of SN-38, was decreased in 10 μM prodrug 1 treated cells (Figure 4b). This suggests that chemo-resistance against SN-38 could be overcome by our newly synthesized prodrug (**1**).

The expression levels of cytochrome C (Cyt C) and BAX, mitochondria- and ER-mediated apoptotic genes, cell-death receptors (FADD), and caspase apoptotic genes (Caspase-3 and -9) were increased, respectively, whereas the expression of the anti-apoptotic p53 was decreased subsequent to prodrug **1** treatment (Figure 4b). Particularly BAX, having an important Ca^{2+} channel regulating role in mitochondria as well as the ER,[39] is thought to play a pivotal role in the mechanism underlying prodrug **1**'s mode of action, briefly schematically outlined in Figure 4c.

In conclusion, this is the first study reporting a DDS system bearing a NQO1 triggering unit successfully inducing mitochondria- and ER-mediated apoptosis, presumably caused by BAX up-regulation. The combination of the enzymatic activation and biotin-based targeting provides a high level of specificity for cancer cells relative to healthy cells *in vitro*, an effect that is mirrored *in vivo* in the case of A549 mouse xenografts, and mechanistic studies have demonstrated a reduced drug resistance induction response. We thus propose that the present theranostic strategy can be extended beyond the specific components present in prodrug **1** to provide a new, generalizable approach to the development of rationally designed small molecular cancer chemotherapeutics.

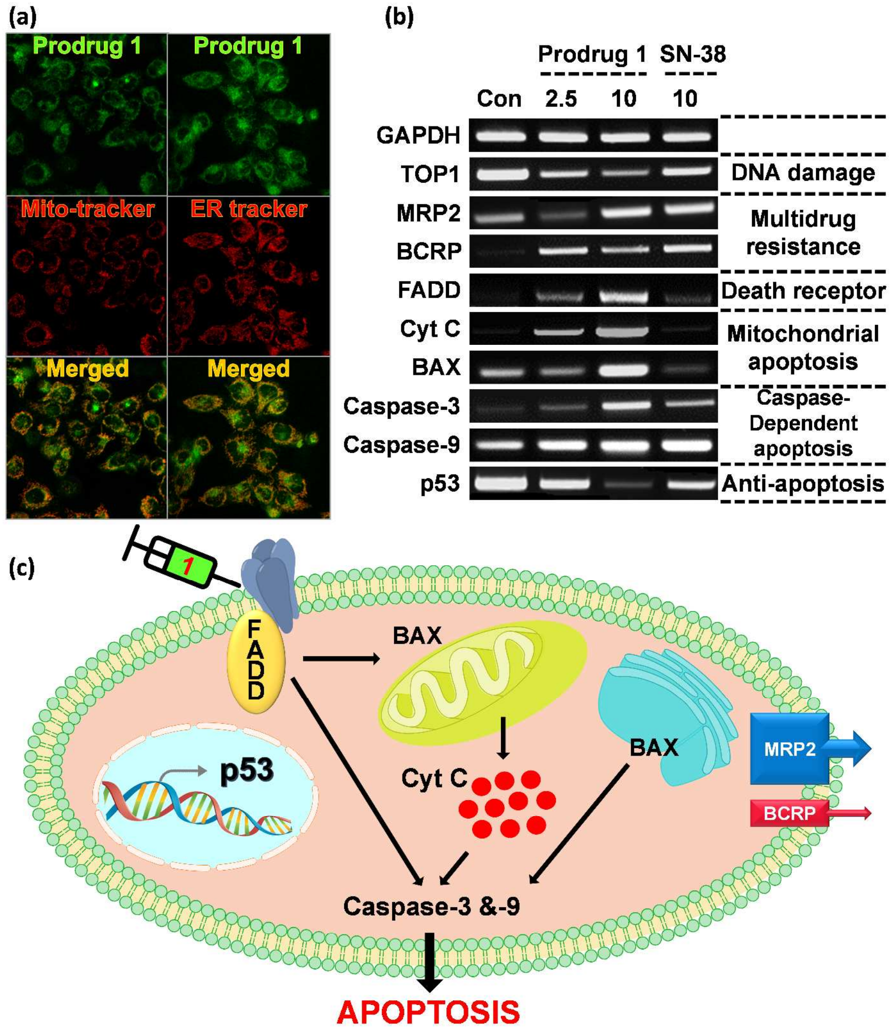

Figure 4. Mechanism of prodrug **1**-induced apoptosis. (a) Subcellular localization of **1**. Fluorescent images of Mito-tracker Red FM (*Ex/Em* 581⁄644 nm) and ER-tracker Red (*Ex/Em* 587⁄615) in A549 cells. The HeLa cells were treated with 10 μM prodrug **1** for 24 h. Cells treated with 10 μM SN-38 were used as controls. (b) Reverse-transcription polymerase chain reaction (PCR) analysis of apoptotic gene expression induced by prodrug **1**. (c) Schematic mode of action of prodrug **1**. The sequential mode of apoptotic action of prodrug **1** through ER- and mitochondria-mediated cell death and DNA integration.

Experimental section

Materials and methods for the synthesis. The reagents used in this study were purchased from Alfa-Aesar, Aldrich, TCI, Carbosynth, Duksan, and Acros and used without further purification. Silica gel 60 (Merck, 0.040-0.063 mm) was used for column chromatography and Merck 60 F254 silica gel plates were used for analytical thin-layer chromatography. ^{1}H and ^{13}C NMR spectra were recorded in $CDCl_3$ on a Varian instrument. Reverse-phase HPLC experiments were performed on a VDSpher 100 C18-E column (5μm, 250 × 4.6 mm) with a Young Lin HPLC system (YL9100) using a mobile phase consisting of a binary gradient of solvent A (water with 0.5% *v*/*v* TFA) and solvent B (acetonitrile with 0.5% *v*/*v* TFA). ESI mass spectrometric analyses were carried out using an LC/MS-2020 Series (Shimadzu) instrument.

Synthesis of compound 1. Compound **2** (20 mg, 0.024 mmol), **9** (7.56 mg, 0.024 mmol), $CuSO_4 \cdot 5H_2O$ (3 mg, 0.012 mmol), and sodium ascorbate (2.39 mg, 0.012 mmol) were mixed and stirred in DMF (5 mL) at room temperature under argon for 12 h. After completion of reaction, the solvent was removed and the reaction mixture was purified by HPLC to obtain the product, 23 mg (86% yield). ^{1}H NMR ($CDCl_3$, 400 MHz): δ 8.21 (d, J = 9.24 Hz, 1H), 7.90 (s, 1H), 7.78 (s, 1H), 7.64 – 7.60 (m, 1.5H), 7.27 (s, 0.5H), 7.18 (s, 1H), 7.09 – 6.98 (m ,2H), 6.41 (s, 1H), 6.05 (s, 1H), 5.73 (d, J = 16.4 Hz, 1H), 5.31 – 5.25 (m, 5H), 4.64 (t, J = 5 Hz, 1H), 4.53 – 4.48 (m, 2H), 4.34 – 4.31 (m, 1H), 3.26 (s, 1H), 3.16 – 3.12 (m, 2H), 2.89 (dd, J = 12.8, 4.76 Hz, 1H), 2.27 (t, J = 6.96 Hz, 1H), 2.17 (d, J = 16.16 Hz, 3H), 1.92 – 1.85 (m, 5H), 1.68 – 1.53 (m, 5H), 1.47 (s, 4H), 1.38 (t, J = 7.48 Hz, 5H), 1.01 (t, J = 7.12 Hz, 3H), 0.88 – 0.83 (m, 9H) ppm. ^{13}C NMR ($CDCl_3$, 100 MHz): δ 191.16, 187.58, 174.07, 173.11, 170.98, 164.62, 157.82, 153.47, 152.17, 150.58, 149.97, 149.86, 147.52, 146.88, 145.80, 144.12, 143.04, 140.35, 139.31, 138.78, 133.79, 132.33, 127.66, 127.58, 124.92, 123.76, 123.33, 122.02, 118.92, 114.50, 114.43, 98.51, 73.06, 70.32, 66.43, 62.89, 62.43, 62.18, 60.71, 55.60, 49.69, 49.55, 47.34, 40.58, 38.54, 37.29, 33.56, 32.95, 32.14, 31.76, 31.15, 30.24, 29.91, 29.57, 28.96, 28.37, 28.22, 27.29, 24.67, 23.38, 22.91, 19.94, 14.57, 14.34, 14.22, 12.87, 12.34, 8.05 ppm. ESI-MS: *m/z* calcd for $C_{59}H_{63}N_7O_{15}S$ (M+Na): 1164.40; detected 1164.0.

Synthesis of compound 2. Compound **3** (100 mg, 0.24 mmol) was dissolved in distilled DCM (10 mL) in round bottom flask and placed in an ice bath under nitrogen gas. Phosgene in toluene (2.00 mL) was added with a syringe. Triethylamine (25 μL, 0.3 mmol) was slowly added with a syringe. After 1 h stirring, the mixture was evaporated to remove the remaining phosgene gas. 7-Ethyl-10-hydroxycamptothecin (86 mg, 0.21 mmol) and triethylamine (25 μL, 0.3 mmol) dissolved in 5 mL of DMF were added. After 12 h the mixture was washed with an aqueous 1*N* HCl solution with ethyl acetate. The organic layer was dried over $MgSO_4$ and concentrated *in vacuo*. Purification by column chromatography yielded 56 mg (28% yield) of compound **2**. ^{1}H NMR ($CDCl_3$, 300 MHz): δ 8.28 (d, J = 9.24 Hz, 1H), 7.91 (d, J = 2.37 Hz, 1H), 7.73 (s, 1H), 7.66 (dt, J = 9.21 Hz, 2.52 Hz, 1H), 7.32 (dd, J = 8.43 Hz, 2.1 Hz, 1H), 7.17 – 6.99 (m, 3H), 5.76 (d, J = 16.35 Hz, 1H), 5.34 – 5.23 (m, 5H), 4.67 (t, J = 2.28 Hz, 2H), 3.28 (s, 2H), 3.17 (q, J = 7.68 Hz, 2H), 2.52 (t, J = 2.88 Hz, 1H), 2.17 (s, 3H), 2.01 (s, 1H), 1.93 – 1.89 (m, 8H), 1.39 (t, J = 7.71 Hz, 3H), 1.02 (t, J = 7.41 Hz, 3H) ppm. ^{13}C NMR ($CDCl_3$, 75 MHz): δ 191.03, 187.72, 173.91, 170.92, 170.88, 157.93, 153.46, 152.24, 152.19, 151.79, 151.04, 150.16, 150.14, 149.83, 149.46, 147.21, 146.69, 146.32, 146.31, 143.15, 140.12, 139.31, 138.70, 133.43, 132.04, 128.23, 127.80, 127.68,127.63, 127.61, 125.27, 124.06, 123.56, 122.49, 118.98, 114.75, 114.42, 114.24, 99.39, 77.88, 76.51, 73.04, 70.11, 66.33, 56.74, 49.87, 47.42, 38.69, 31.78, 29.15, 29.12, 23.47, 14.55, 14.19, 12.90, 12.35, 8.00 ppm. ESI-MS: *m/z* calcd for $C_{47}H_{44}N_2O_{12}$ (M+Na): 851.28, (M+K): 867.25; detected 851.0, 867.0, respectively.

Synthesis of compound 3. Compound **4** (100 mg, 0.19 mmol) was dissolved in THF, then cooled in an ice-water bath. *p*-Toluenesulfonic acid (18 mg, 0.095 mmol) was added and the reaction warmed to room temperature. After 8 hours, the reaction was extract with DCM and water. The organic layer was dried over $MgSO_4$ and concentrated *in vacuo*. Purification by column chromatography yielded 37 mg (48% yield) of **3**. ^{1}H NMR ($CDCl_3$, 300 MHz): δ 7.15 (dd, J = 8.4 Hz, 2.04 Hz, 1H), 7.02 (d, J = 8.4 Hz, 1H), 6.97 (d, J = 1.98 Hz, 1H), 4.62 – 4.56 (m, 4H), 3.25 (s, 2H), 2.48 (t, J = 2.4 Hz, 1H), 2.16 (s, 3H), 1.92 – 1.88 (m, 6H), 1.52 (s, 6H) ppm. ^{13}C NMR ($CDCl_3$, 75 MHz): δ 171.03, 152.33, 148.59, 143.21, 140.07, 139.16, 138.60, 135.10, 125.46, 123.12, 120.19, 114.35, 112.78, 78.19, 76.22, 64.53, 56.79, 47.44, 38.67, 29.93, 29.10, 14.53, 14.37, 12.89, 12.33 ppm. ESI-MS: *m/z* calcd for $C_{24}H_{26}O_6$ (M+K): 449.14; detected 449.0.

Synthesis of compound 4. EDC·HCl (106 mg, 0.68 mmol) was added to a solution of **5** (100 mg, 0.34 mmol), **8** (73 mg, 0.41 mmol) and DMAP (83 mg, 0.68 mmol) in DCM (5 mL) at room temperature. After 12 h the mixture was washed with an aqueous 1*N* HCl solution, the organic layer was dried with $MgSO_4$, filtered and concentrated *in vacuo*. Purification by column chromatography yielded 112 mg (63% yield) of **4**. ^{1}H NMR ($CDCl_3$, 300 MHz): δ 7.12 (dd, J = 8.43 Hz, 2.1 Hz, 1H), 7.02 (d, J = 8.43 Hz, 1H), 6.92 (d, J = 2.1 Hz, 1H), 4.63 (s, 2H), 4.62 (d, J = 2.4 Hz, 2H), 3.26 (s, 2H), 2.47 (t, J = 2.37 Hz, 1H), 2.16 (s, 3H), 1.92 (s, 3H), 1.89 (d, J = 1.11 Hz, 3H), 1.53 (s, 6H), 0.91 (s, 9H), 0.07 (s, 6H) ppm. ^{13}C NMR ($CDCl_3$, 75 MHz): δ 191.16, 187.72, 170.92, 152.50, 148.08, 143.26, 148.08, 143.26, 140.01, 139.00, 138.51, 135.67, 124.34, 121.06, 114.24, 76.03, 64.27, 58.89, 47.48, 38.65, 29.06, 26.14, 14.50, 12.88, 12.31 ppm. ESI-MS: *m/z* calcd for $C_{30}H_{40}O_6Si$ (M+Na); 547.25; detected 547.0.

Synthesis of compound 5. Compound **6** (100 mg, 0.56 mmol) was dissolved in dry DCM, then cooled in an ice-water bath. Imidazole (45 mg, 0.67 mmol) and *tert*-butyldimethylsilyl chloride (101 mg, 0.67 mmol) were added and the reaction warmed to room temperature. After 8 hours, the reaction was diluted with ether (50 mL) and washed with saturated NH_4Cl (50 mL) and brine (25 mL). The organic layer was dried over $MgSO_4$ and concentrated *in vacuo*. Purification by column chromatography yielded 123 mg (75% yield) of **5**. ^{1}H NMR ($CDCl_3$, 300 MHz): δ 6.96 – 6.92 (m, 3H), 5.82 (s, 1H), 4.72 (d, J = 2.37 Hz, 2H), 4.66 (s, 2H), 2.56 (t, J = 2.4 Hz, 1H), 0.96 (s, 9H), 0.12 (s, 6H) ppm. ^{13}C NMR ($CDCl_3$, 75 MHz): δ 146.03, 143.68, 136.12, 117.66, 113.36, 112.78, 78.32, 76.17, 64.63, 57.16, 26.04, 18.47 ppm.

Synthesis of compound 6. To a solution of **7** (200 mg, 1.13 mmol) in methanol (3 mL) and water (100 µL) $NaBH_4$ (37 mg, 3.40 mmol) was added while stirring. The reaction mixture was stirred at room temperature for 4 h, at which time MeOH (2 mL), water (1 mL) and solid NH_4Cl (until neutral pH) were subsequently added to the suspension. The resulting suspension was stirred for 5 min, diluted with EtOH, and evaporated to dryness. Purification by column chromatography yielded 179 mg (89% yield) of **6**. ^{1}H NMR ($CDCl_3$, 300 MHz): δ 6.95 – 6.92 (m, 2H), 6.84 (dd, J = 8.22 Hz, 1.98 Hz, 1H), 4.73 (d, J = 2.37 Hz, 2H), 4.56 (s, 2H), 2.55 (t, J = 2.4 Hz, 1H) ppm.

Synthesis of compound 7. This compound was synthesized, according to a previously reported procedure[35] with a 60% yield.

Synthesis of compound 8. This compound was synthesized, according to a previously reported procedure[36] in two steps with an 82% overall yield.

Synthesis of compound 9. This compound was synthesized, according to a previously reported procedure[8] in two steps with a 72% overall yield.

Cell culture. Two biotin receptor-positive cell lines; human lung carcinoma cells (A549) and human cervical cancer cells (HeLa) were purchased from the Korean Cell Line Bank (Seoul, Republic of Korea). Two biotin receptor-negative normal cell lines; human normal fibroblast cells obtained from fetal lung (WI-38 cells) or neonatal foreskin (BJ) cells were purchased from the Korean Cell Line Bank (Seoul, Republic of Korea) and Modern Cell & Tissue Technologies (MCTT, Seoul, Republic of Korea). The cells were cultured in either Dulbecco's Modified Eagle's Medium (DMEM, GIBCO BRL) or Roswell Park Memorial Institute medium (RPMI-1640, GIBCO BRL, Grand Island, NY, USA) supplemented with 10% fetal bovine serum (FBS, GIBCO), and 1% penicillin and streptomycin (GIBCO), at 37 $^{\circ}$C in a humidified atmosphere containing 5% of CO_2. When the cell density reached 70–80% of confluence, sub-culturing was considered complete. The medium was changed approximately every 3 to 4 days.

Cytotoxicity analysis. The normal cells lines (WI-38 and BJ) and biotin receptor-positive cell lines were used to evaluate the cytotoxicity of prodrug **1**. Prior to test, the cells were washed two times with PBS and then exchanged into FBS-free culture medium. Actual cell viability was monitored by using a 3-(4,5-dimethylthiazol-2-yl)-2,5-diphenyltetrazolium bromide (MTT; Life Technologies, Carlsbad, CA, USA) assay in accordance with the manufacturer's instructions. Briefly, 1.5 × 104 cells were seeded in each well in a 96-well plate. The next day, the culture medium was removed and exchanged with fresh medium (100 µL) containing different concentrations (0, 2.5, 10, or 50 µM) of prodrug **1**. Additionally, SN-38 (10, 25, 50, 100, 200 µM) in 100 µL medium was replaced for comparing the cytotoxicity of prodrug **1**. Cells were incubated at 37 °C for 24 h. Then, a 12 mM MTT solution (150 μL) was added to each well. For negative controls, 150 μL of the MTT stock solution or distilled water were added per well in the absence of prodrug **1**, i.e., to 150 μL of the medium alone. The medium of each well was removed after 24h incubation, and 50 μL of DMSO was added. The resulting suspension was mixed thoroughly for 15 min and the absorbance was monitored using a microplate spectrophotometer at 540 nm (PowerWave XS, Bio-Tek, Winooski, VT, USA).

***In vitro* cell imaging.** Prior to fluorescent imaging, cells were seeded in 35-mm confocal dishes (glass bottom dish, SPL) and allowed to stabilize for 48 h. The cell density was 2.0×10^6 in the 35-mm confocal dish. The A549 and HeLa cells were treated with prodrug **1**. The cells were incubated with media containing 10 μM prodrug **1** (added in 10 μL of DMSO in 2 mL of medium per 35-mm dish) for 24 h at 37 °C in 5% CO_2. Then, 1 mL of PBS was added twice to wash the cells, prior to adding FBS-free DMEM or RPMI 1640 culture medium. Then prodrug **1** was treated for 24 h. The cells were again washed twice with PBS, and florescent images were taken under a confocal laser scanning microscope (Carl-Zeiss LSM 5 Exciter, Oberko, Germany), which was equipped with a 405-nm Argon laser and 500-nm pass filter. Analysis of co-localization was performed using Mito-tracker Red FM (Thermo Fisher, New Hampshire, USA, Ex/Em 581⁄644 nm) or ER-tracker Red (Thermo Fisher, Ex/Em 587⁄615) according to the manufacturer’s instructions. Stained cells were visualized by means of a Zeiss LSM510 laser scanning confocal microscope using the cyc3.5 filter (Carl Zeiss, Oberkochen, Germany).

RT-PCR. Total RNA from the cells was isolated using the TRIzol Reagent (Invitrogen). The RNA was reverse-transcribed using a reverse transcription system (Promega, Madison, WI). EXTaq polymerase (Takara, Japan) was used for PCR amplification of different genes, under the following cycling conditions: 94 °C for 5 min; then 35 cycles of 94 °C for 30 s, 50–57 °C for 30 s, and 72 °C for 30 s; with final incubation at 72 °C for 10 min. The primers and PCR conditions are shown in the supplemental information.

Mouse xenograft model. To examine the chemotherapeutic effects and to obtain images of prodrug 1 *in vivo*, 6-week-old BALB/c nude mice from RaonBio (Kayonggido, Yonginsi, South Korea) were used as follows: (n = 4 per treatment). Before the various the animals were stored in an animal facility they were allowed to acclimate for 48 h and maintained as per the guidelines of the Care and Use of Laboratory Animals published by the National Institutes of Health (Bethesda, MD, USA). The animals were housed in cages and provided with water *ad libitum* and sterilized food, and maintained in a 12 h light/dark cycle with 30–40% humidity at room temperature (21 ± 2 $^{\circ}$C). The 354234-matrigel (BD, San Jose, California, USA) was mixed with approximately 5.0×10^6 A549 cells and subcutaneously injected into the right and left flanks of the mice.

***In vivo* administration of prodrug 1.** To assess the diagnostic effects of prodrug 1 *in vivo*, the fluorescent intensity of prodrug **1** in mouse sera was detected after 3 mg/kg prodrug **1** in 0.1 mL PBS injected two times a week for three weeks. Xenograft mice were subject to a single tail vein injection with prodrug **1**. The fluorescent images were obtained by using a Maestro™ *In vivo* Fluorescence Imaging System (Maestro, CRi Inc., Woburn, MA, USA). To compare therapeutic effects, the same concentration of SN-38 was injected for four weeks. Total tumor weights were measured at the end of the experiment. Animals were terminated by CO_2 gas.

Statistical analysis. The mean of each groups and standard error of the mean (SEM) were calculated from three independent experiments carried out in triplicate. ANOVA (One-way analysis of variance) in the SAS software (version 8.2, Cary) was performed to evaluate the statistical significance of differences between groups. Paired Student's t tests were performed to compare the means when ANOVA indicated a significant difference. P values <0.05 were assumed to denote statistical significance.

Acknowledgment

This work was supported by The Ministry of Science, ICT & Future Planning (MSIP) of National Research Foundation of Korea (No. 2009-0081566 for JSK, No. 2012M3A9B4028636 for J-HK, and No. 2015R1C1A1A02036905 for JH), a Korea University Grant (JH and PV).

References

1. Cairns, R., Papandreou, I., and Denko, N. (2006) Overcoming physiologic barriers to cancer treatment by molecularly targeting the tumor microenvironment. *Mol. Cancer Res. 4*, 61-70.
2. Zhang, Q., Ko N. R., and Oh, J. K. (2012) Recent advances in stimuli-responsive degradable block copolymer micelles: synthesis and controlled drug delivery applications. *Chem. Commun. 48*, 7542-7552.
3. Chang, E. L., Schwartz, B. D., Draffan, A. G., Banwell M. G., and Willis, A. C. (2015) pH-Responsive Drug-Delivery Systems. *Chem. Asian J. 10*, 284-305.
4. Xu, Q., He, C., Xiao, C., and Chen, X. (2016) Reactive Oxygen Species (ROS) Responsive Polymers for Biomedical Applications. *Macromol. Biosci.* doi: 1002/mabi.201500440
5. Lee, M. H., Sessler, J. L., and Kim, J. S. (2015) Disulfide-Based Multifunctional Conjugates for Targeted Theranostic Drug Delivery. *Acc. Chem. Res*. *48*, 2935-2946.
6. Wu, X., Sun, X., Guo, Z., Tang, J., Shen, Y., James, T. D., Tian, H., and Zhu, W. (2014) In Vivo and in Situ Tracking Cancer Chemotherapy by Highly Photostable NIR Fluorescent Theranostic. *J. Am. Chem. Soc*. *136*, 3579-3588.
7. Maiti, S., Park, N., Han, J. H., Jeon, H. M., Lee, J. H., Bhuniya, S., Kang, C., and Kim, J. S. (2013) Gemcitabine-Coumarin-Biotin Conjugates: A Target Specific Theranostic Anti-Cancer Prodrug. *J. Am. Chem. Soc*. *135*, 4567-4572.
8. Yang, Z., Lee, J. - H., Jeon, H. M., Han, J. H., Park, N., He, Y., Lee, H., Hong, K. S., Kang, C., and Kim, J. S. (2013) Folate-Based Near-Infrared Fluorescent Theranostic Gemcitabine Delivery. *J. Am. Chem. Soc*. *135*, 11657-11662.
9. Bhuniya, S., Maiti, S., Kim, E. - J., Lee, H., Sessler, J. L., Hong, K. S., and Kim, J. S. (2014) An Activatable Theranostic for Targeted Cancer Therapy and Imaging. *Angew. Chem. Int. Ed. 53*, 4469-4474.
10. Lee, M. H., Kim, J. Y., Han, J. H., Bhuniya, S., Sessler, J. L., Kang, C., and Kim, J. S. (2012) Direct Fluorescence Monitoring of the Delivery and Cellular Uptake of a Cancer-Targeted RGD Peptide-Appended Naphthalimide Theragnostic Prodrug. *J. Am. Chem. Soc*. *134*, 12668-12674.
11. Tedeschi, G., Chen, S., and Massey, V. J. (1995) DT-diaphorase. Redox potential, steady-state, and rapid reaction studies. *Biol. Chem*. *270*, 1198-1204.

12. Hettiarachchi, S. U., Prasai, B., and McCarley, R. L. (2014) Detection and Cellular Imaging of Human Cancer Enzyme Using a Turn-On, Wavelength-Shiftable, Self-Immolative Profluorophore. *J. Am. Chem. Soc*. *136*, 7575-7578.

13. Mendoza, M. F., Hollabaugh, N. M., Hettiarachchi, S. U., and McCarley, R. L. (2012) Human NAD(P)H:Quinone Oxidoreductase Type I (hNQO1) Activation of Quinone Propionic Acid Trigger Groups. *Biochemistry 51*, 8014–8026.

14. Cho, H., Bae, J., Garripelli, V. K., Anderson, J. M., Jun, H. - W., and Jo, S. (2012) Redox-sensitive polymeric nanoparticles for drug delivery. *Chem. Commun*. *48*, 6043–6045.

15. Volpato, M., Abou-Zeid, N., Tanner, R. W., Glassbrook, L. T., Taylor, J., Stratford, I., Loadman, P. M., Jaffar, M., and Phillips, R. M. (2007) Chemical synthesis and biological evaluation of a NAD(P)H:quinone oxidoreductase-1 targeted tripartite quinone drug delivery system. *Mol. Cancer Ther*. *6*, 3122-3130.

16. Ong, W., Yang, Y., Cruciano, A. C., and McCarley, R. L. (2008) Redox-Triggered Contents Release from Liposomes. *J. Am. Chem. Soc. 130*, 14739–14744.

17. Silvers, W. C., Prasai, B., Burk, D. H., Brown, M. L., and McCarley, R. L. (2013) Profluorogenic Reductase Substrate for Rapid, Selective, and Sensitive Visualization and Detection of Human Cancer Cells that Overexpress NQO1. *J. Am. Chem. Soc*. *135*, 309–314.

18. Silvers, W. C., Payne, A. S., and McCarley, R. L. (2011) Shedding light by cancer redox—human NAD(P)H:quinone oxidoreductase 1 activation of a cloaked fluorescent dye. *Chem. Commun*. *47*, 11264–11266

19. Danson, S., Ward, T. H., Butler, J., and Ranson, M. (2004) DT-diaphorase: a target for new anticancer drugs. *Cancer Treat. Rev*. *30*, 437-449.

20. Cresteil, T., and Jaiswal, A. K. (1991) High levels of expression of the NAD(P)H:quinone oxidoreductase (NQO1) gene in tumor cells compared to normal cells of the same origin. *Biochem. Pharmacol. 42*, 1021-1027.

21. Lewis, A. M., Ough, M., Hinkhouse, M. M., Tsao, M. S., Oberley, L. W., and Cullen, J. J. (2005) Targeting NAD(P)H:quinone oxidoreductase (NQO1) in pancreatic cancer. *Mol. Carcinog. 43*, 215-224.

22. Schlager, J. J., and Powis, G. (1990) Cytosolic NAD(P)H:(quinone-acceptor)oxidoreductase in human normal and tumor tissue: effects of cigarette smoking and alcohol. *Int. J. Cancer 45*, 403-409.

23. Yang, Y., Zhang, Y., Wu, Q., Cui, X., Lin, Z., and Liu, S. (2014) Clinical implications of high NQO1 expression in breast cancers. *J. Exp. Clin. Cancer Res. 33*, 14.

24. Rosario, I. B., Consuelo, G. - D., Francisco, N., Francisco, J. A., and Jose, M. V. (2001) Expression of NAD(P)H:Quinone Oxidoreductase 1 in HeLa Cells. *J. Bio. Chem. 48*, 44379-44384.

25. Jaracz, S., Chen, J., Kuznetsova, L. V., and Ojima, I. (2005) Recent advances in tumor-targeting anticancer drug conjugates. *Bioorg. Med. Chem. 13*, 5043-5054.

26. Leamon, C. P., and Reddy, J. A. (2004) Folate-targeted chemotherapy. *Adv. Drug Deliv. Rev. 56*, 1127-1141.

27. Lu, Y., and Low, P. S. (2002) Folate-mediated delivery of macromolecular anticancer therapeutic agents. *Adv. Drug Deliv. Rev. 54*, 675-693.

28. Wu, Y., Wang, X., Chang, S., Lu, W., Liu, M., and Pang, X. (2016) β-Lapachone Induces NQO1- and Oxidative Stress-Dependent Hsp90 Cleavage and Inhibits Tumor Growth and Angiogenesis. *J. Pharmacol. Exp. Ther.* doi: 10.1124/jpet.116.232694.

29. Liu, K., Jin, B., Wu, C., Yang, J., Zhan, X., Wang, L., Shen, X., Chen, J., Chen, H., and Mao, Z. (2015) NQO1 Stabilizes p53 in Response to Oncogene-Induced Senescence. *Int. J. Biol. Sci. 11*, 762-771.

30. Russell-Jones, G., McTavish, K., McEwan, J., Rice, J., and Nowotnik, D. (2004) Vitamin-mediated targeting as a potential mechanism to increase drug uptake by tumours. *J. Inorg. Biochem. 98*, 1625-1633.

31. Ren, W. X., Han, J., Uhm, S., Jang, Y. J., Kang, C., and Kim, J. S. (2015) Recent development of biotin conjugation in biological imaging, sensing, and target delivery. *Chem. Commun. 51*, 10403-10418.

32. Pommier, Y. (2006) Topoisomerase I inhibitors: camptothecins and beyond. *Nat. Rev. Cancer 6*, 789-802.

33. Kaneda, N., Nagata, H., Funita, T., and Yokokura, T. (1990) Metabolism and pharmacokinetics of the camptothecin analogue CPT-11 in the mouse. *Cancer Res. 50*, 1715-1720.

34. Liu, P., Xu, J., Yan, D., Zhang, P., Zeng, F., Li, B., and Wu, S. (2015) A DT-diaphorase responsive theranostic prodrug for diagnosis, drug release monitoring and therapy. *Chem. Commun. 51*, 9567-9570.

35. Wei, Q., Seward, G. K., Hill, P. A., Patton, B., Dimitrov, I. E., Kuzma, N. N., and Dmochowski, I. J. (2006) Designing 129Xe NMR Biosensors for Matrix Metalloproteinase Detection. *J. Am. Chem. Soc. 128*, 13274-13283.

36. Rohde, R. D., Agnew, H. D., Yeo, W. - S., Bailey, R. C., and Heath, J. R. (2006) A Non-Oxidative Approach toward Chemically and Electrochemically Functionalizing Si(111). *J. Am. Chem. Soc. 128*, 9518-9525.

37. Yilmaz, A., Mohamed, N., Patterson, K. A., Tang, Y., Shilo, K., Villalona-Calero, M. A., Davis, M. E., Zhou, X., Frankel, W., Otterson, G. A. *et al.* (2014) Increased NQO1 but not c-MET and survivin expression in non-small cell lung carcinoma with KRAS mutations. Int. J. Environ. *Res. Public Health. 11*, 9491-9502.

38. Nakanishi, T., and Ross, D. D. (2012) Breast cancer resistance protein (BCRP/ABCG2): its role in multidrug resistance and regulation of its gene expression. *Chin. J. Cancer 31*, 73-99.

39. Lee, H., Park, M. - T., Choi, B. - H., Oh, E. - T., Song, M. - J., Lee, J., Kim, C., Lim, B. U., and Park, H. J. (2011) Endoplasmic reticulum stress-induced JNK activation is a critical event leading to mitochondria-mediated cell death caused by β-lapachone treatment. *PLoS One. 6*, e21533.

Table of Contents Graphic